Geophysical Journal International

Geophys. J. Int. (2013) doi: 10.1093/gji/ggt230

Geophysical Journal International Advance Access published July 4, 2013

Lightning-induced remanent magnetization—the Vredefort impact structure, South Africa

Johanna Salminen,[1,2] Lauri J. Pesonen,[2] Kari Lahti[3] and Kari Kannus[3]

[1]*Department of Geology and Geophysics, Yale University, P.O. Box* 208109*, New Haven, CT* 06520-8109*, USA. E-mail: Johanna.m.salminen@helsinki.fi*
[2]*Department of Physics, University of Helsinki, P.O. Box* 64*, FI-*00014 *University of Helsinki, Finland*
[3]*Department of Electrical Energy Engineering, Tampere University of Technology, P.O. Box* 692*, FI-*33101 *Tampere, Finland*

Accepted 2013 June 5. Received 2013 June 4; in original form 2012 October 3

SUMMARY

Earlier studies at the large Vredefort impact structure since 1960 have shown that values of natural remanent magnetizations (NRMs) and, hence, Koenigsberger's Q values (ratio of remanent over induced magnetization), for different rock lithologies are elevated compared to the values for similar rock types around the world. Three origins for the high Q values have been suggested, namely shock by meteorite impact, enhanced plasma field and lightning strikes. We have studied whether laboratory lightning experiments can produce enhanced NRMs in the Vredefort target rocks. For comparison, we also included rocks from the Johannesburg dome, which is not a meteorite impact site. The results revealed increased NRMs, susceptibility and Q values of the rocks from both Vredefort and Johannesburg domes.

Rock magnetic measurements and scanning electron microscope analyses of lightning pulsed and unpulsed samples showed that the lightning included changes in magnetic properties of the rocks. We suggest that in some samples lightning have changed magnetic mineralogy by oxidizing magnetite to maghemite. Indication of this oxidation came from the low-temperature variation of the remanent magnetization where we observed several hallmarks of maghemitization in samples treated by lightning strikes. Further indications of mineralogical changes include increased Curie points above the magnetite's Curie point (580 °C) and appearance of pronounced lower temperature (200–400 °C) phases in susceptibility versus temperature curves. These changes are interpreted to indicate partially oxidized magnetite (maghemitization) coupled with grain fragmentations and by this way grain size reduction. High-temperature hysteresis and REM (= NRM/saturation isothermal remanent magnetization) studies support these conclusions. Our results were analogous with the ones for lodestones and protolodestones where partially oxidized magnetite is thought to make magnetization more intense.

Key words: Magnetic mineralogy and petrology; Remagnetization; Rock and mineral magnetism.

1 INTRODUCTION

The Vredefort impact structure in South Africa with estimated diameter of 250 km (Henkel & Reimold 1998) and age of 2023 ± 4 (2σ) Ma (Kamo *et al.* 1996) is considered the largest and the oldest impact structure on the Earth (Gibson & Reimold 2001, 2008). Rock magnetic and palaeomagnetic studies on the Vredefort crater started already in the 1960s (Hargraves 1961, 1970) and they have been ongoing ever since (e.g. Jackson 1982; Layer *et al.* 1988, 1989a,b; Hattingh 1989, 1999; Hart *et al.* 1995, 2000; Henkel & Reimold 1998; Cloete *et al.* 1999; Carporzen *et al.* 2005, 2006; Muundjua *et al.* 2007; Salminen *et al.* 2009). These studies show that values of natural remanent magnetizations (NRMs) and, hence, Koenigsberger's Q values (ratio of remanent over induced magnetization), for a variety of rock lithologies in the Vredefort are elevated compared to the values for similar rock types found elsewhere in the world. In the case of Vredefort, the high Q values are associated with random directions of NRM even though they are magnetically stable against demagnetization (Salminen *et al.* 2009). It has been suggested that the source for elevated NRMs is related to an impact event (high pressure and temperature) in which an ultra-small single-domain (SD) magnetite crystallized along shock generated planar deformation features (Hart *et al.* 1995, 2000; Cloete *et al.* 1999). Carporzen *et al.* (2005) further proposed that a plasma field produced by the impact event generated small-wavelength magnetic fields of high intensity which not only produced high NRMs but also randomized the directions of NRM. The latter suggestion does not take in to an account that the present erosional level of the Vredefort impact structure is *ca.* 5–10 km and the plasma field would not have been able to penetrate so deep (Turtle & Pierazzo 1998; Crawford & Schultz 1999). Moreover, the cooling time of the impact structure after the meteorite hit is much longer (several hundreds of thousands of years; e.g. Ivanov 2005) than the lifetime of a plasma field, which is from seconds to minutes (e.g. Turtle & Pierazzo 1998; Crawford & Schultz 1999). Besides the rock magnetic and palaeomagnetic results of Salminen *et al.* (2009) show that there is no concentration of elevated Q values near the centre of the structure nor do they decay radially away, as it should be if they were of impact origin. Yet the elevated Q values are also seen in samples from the Johannesburg dome *ca.* 120 km north from the Vredefort dome and thus outside of the impact effects. Finally, a correlation between hysteresis data and elevated Q values of the basement rocks was not observed, as would be expected if the ultra-fine particles in the PDFs were the sole carriers of the high Q values. These arguments collectively rule out the direct connection of elevated NRM to the impact event in the Vredefort.

Carporzen *et al.* (2012) have recently proposed that the high Q values in the Vredefort dome samples could represent effects of lightning strikes that was already discussed as one of the possible sources by Salminen *et al.* (2009), but excluded due to lack of further test. To prove lightning strike theory, Carporzen *et al.* (2012) drilled two 10-m cores in the Vredefort and showed that the abnormal magnetic properties vanish within 0.5 m from the surface. This indicates that they are not due to impact-generated plasma field, but rather produced by lightning strikes. Lightning is a very common phenomenon in South Africa: the average current lightning density is 23 flashes km^{-2} yr^{-1}; (Christian *et al.* 2003). The lightning activity maps produced by NASA (http://geology.com/articles/lightning-map.shtml) show that South Africa consists of areas with the highest lightning activity in the world. Lightning is associated with high voltages and electric currents with both positive and negative polarity. An average bolt of negative lightning carries an electric current of 30 kA and transfers 500 MJ of energy to the target where it is hitting. An average bolt of positive lightning carries an electric current of about 10 times (300 kA) the negative one. Lightning strikes rapidly heat the air in its close vicinity to about 20 000 °C. In nature, lightning produced currents last for few tens of milliseconds and thereby generates strong, circular magnetic field, whose axis is oriented perpendicular to current direction. Most lightning flashed include three or four separate upward current pulses space about 50 ms apart (e.g. Krider & Roble 1986). This field will produce a secondary isothermal remanent magnetization (IRM) to the rocks (Verrier & Rochette 2002). IRM can be orders of magnitude higher than typical, thermally (TRM) or chemically (CRM) produced remanences. Generally in the literature, very strong NRMs are interpreted to be caused by lightning (e.g. Graham 1961).

In nature, lodestones, which are pure iron ore bodies, are a known to be magnetically very hard (e.g. Wasilewski 1977, 1979; Banfield *et al.* 1994). Lodestones are iron ores that behave as permanent magnets. Furthermore, iron ores that are capable of being charged strongly to behave as permanent magnets have been defined as protolodestones (Wasilewski 1979). NRM of lodestones and protolodestones is high and more stable against demagnetization than laboratory produced saturation isothermal remanence magnetization (SIRM). A characteristic feature for the protolodestones and lodestones is the high REM ratio (NRM/SIRM ratio) ~0.15–0.7 indicating magnetization in a field much larger than Earth's magnetic field. Typically, these ratios for rocks magnetized in the geomagnetic field are <0.05 (e.g. Wasilewski & Kletetschka 1999). Wasilewksi (1977, 1979) showed that lodestones and protolodestones are magnetically hardened by partial oxidation of magnetite to maghemite. He noted that the microstructure of magnetic grains is highly irregular and there are no lamellae or other ordered structures visible. Later, based on transmission electron microscopy studies, Banfield *et al.* (1994) identified stacking faults and pinning of domain walls, which reduced the effective grain size of mineral, within multidomain grains of lodestones and correlated these with intense stable remanent magnetization. They suggested that both the stacking faults and intense remanent magnetization may be induced in a lightning event.

Since the lightning strikes have been proven to be the source for high remanent magnetization values in Vredefort rocks (Carporzen *et al.* 2012), we wanted to further study the general effects of lightning strikes to rocks. We have simulated lightning strikes with a high-voltage instrument capable of producing 18 kA current (Haefely Test, AG Switzerland; max: 1000 kV) on the sample. Using this instrument, we induced lightning strikes on Archaean basement samples from both the Vredefort and Johannesburg domes and measured several rock magnetic properties to see what changes in rock magnetic properties lightning is causing. Results will be compared to rock magnetic results of untreated sister samples.

2 GEOLOGY, SAMPLING, EXPERIMENTS AND MEASUREMENTS

2.1 Geology and sampling

Gibson & Reimold (2001, 2008) have reviewed the geology of the Vredefort impact structure. The extent of the eroded remnant of this impact structure encompasses the entire Witwatersrand Basin, stretching for 250–300 km between Johannesburg in the northeast and the Welkom goldfields in the southwest. Located roughly in the central part of the basin, the Vredefort dome represents the *ca.* 90-km wide, exhumed root of the central uplift of the structure. Fig. 1 is a schematic geological map showing the simplified geology of the Vredefort dome with sampling sites. The southern and eastern parts of the dome are generally overlain by sedimentary strata and dolerites belonging to the Jurassic (185 Ma) Karoo supergroup.

At the northeastern edge of the Witwatersrand Basin lies the Johannesburg dome, an Archaean terrain composed of granitoids and greenstone remnants with several inliers of Witwatersrand supergroup (WSG) strata (Fig. 1). Immediately north of the Johannesburg dome, the rocks of the 2.6–2.15 Ga Transvaal supergroup dip shallowly to the north beneath the 2.05–2.06 Ga old Bushveld igneous complex (Reimold & Gibson 1996; Cawthorn *et al.* 2006; Eriksson *et al.* 2006).

For this lightning strike study, we used samples taken during the palaeomagnetic field campaign reported in Salminen *et al.* (2009; Fig. 1). Three Archean basement samples (granite and gneiss) with Q values between 2 and 8 (see Table 1) from the Vredefort dome and eight Archean basement samples (gneiss, granite, granodiorite and pegmatite) with Q values 0.4–20 from the Johannesburg dome were studied. We chose the samples from Johannesburg dome since the terrain is not affected by impact shock or as strongly thermally overprinted by the impact generated heat as the rocks of the Vredefort central uplift.

2.2 Experiments

Lightning pulse experiments were performed on standard demagnetized palaeomagnetic cylinders (diameter: 2.54 cm, height: 2.2 cm)

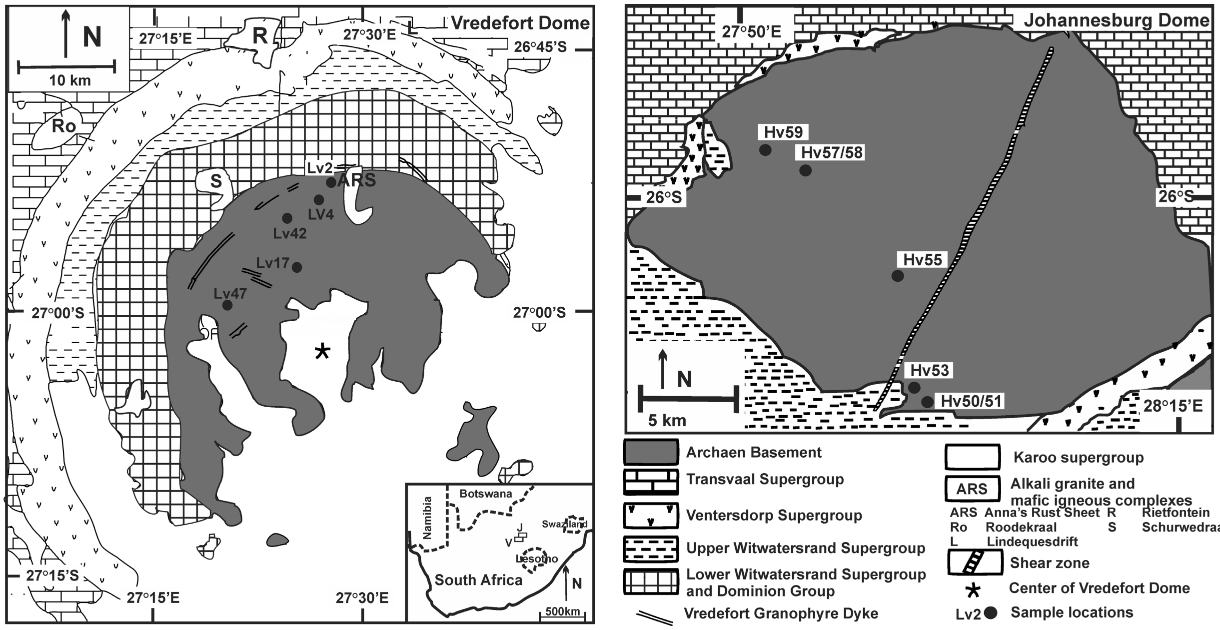

Figure 1. Simplified geology and sampling sites of the Vredefort and Johannesburg domes (modified from Salminen *et al.* 2009).

with a 10-stage lightning impulse generator (Haefely SGS1000-50, Basel, Switzerland) having a maximum charging voltage of 100 kV stage^{-1} and maximum total energy of 50 kJ. The generator was configured to give maximal current impulse to the test circuit with *ca.* 11.5 and 18 kA peak current, in Tampere University of Technology, Finland. The arrangements used during the impulse current applications are illustrated in the schematic Fig. 2. The cylindrical rock samples were placed on large earthed stainless steel plate. A copper-made impulse electrode (diameter 14 mm) perpendicular to the steel plate was then laid on top of the rock sample. When applying an impulse the test voltage first increases at a rate of *ca.* 900 kV μs^{-1} until a flashover takes place at *ca.* 150 kV level over the test sample and current starts to flow through the plasma channel of the flashover arc. The plasma channels form along the surface of the rock sample one side of it. The rise time of the current impulses were *ca.* 2 μs, and the time to half value was *ca.* 9 μs (Fig. 2). With this type of impulse waveforms and at this current level, the size of the current carrying plasma channel is *ca.* 1 cm^2 (Flowers 1943). Polarity of all the applied impulses was positive. Three impulses were applied on all the test samples with presence of Earth's magnetic field of *ca.* 52 μT. The experiment did not leave any visible mark on the rock, which is usually also the case in the field. We are not able to detect by eye those rocks that have been hit by lightning strikes.

Sample orientation was changed between the pulses to simulate the changing direction of lightning strikes in the nature (Fig. 2). These samples are later on called 'pulsed' or 'treated' samples. For every lightning pulsed sample, we have an 'untreated' reference subspecimen from the same palaeomagnetic sample.

2.3 Measurements

Basic petrophysical measurements were carried out for same subsample before and after lightning pulses. Similar rock magnetic measurements were done for both subsample sets ('pulsed' and 'unpulsed') to identify the effects of lightning strikes on rocks. Measurements were done in three different laboratories: Solid Earth Geophysics Laboratory at the University of Helsinki (Finland); Paleomagnetism Laboratory at the Yale University (USA) and at the Institute for Rock Magnetism (IRM) at the University of Minnesota (USA).

Samples were alternating field (AF) demagnetized before and after lightning pulses using 2G SQUID magnetometer (Sand City, CA, USA) or Molspin (ACS Scientific, Carlsbad, CA, USA) AF demagnetizer. Magnetic anisotropy of the AF demagnetized samples was studied by measuring anisotropy of magnetic susceptibility (AMS) using Agico's (Brno, Czech Republic) KLY3-CS kappabrige. SIRM of 1 T was imparted on samples at the IRM and then AF demagnetized using 2G SQUID u-channel magnetometer. High and low-temperature (LT) susceptibility measurements and bulk susceptibility measurements were done using Agico's KLY3-CS and KLY4-CS instruments. The high-temperature measurements were done in argon gas to prevent oxidation. Room temperature hysteresis properties for all and high temperature (from RT to 600 °C in helium atmosphere) for selected samples were measured in IRM using Princeton Measurements vibrating sample magnetometer (VSM; Westerville, OH, USA). LT remanence measurements were done in IRM using a quantum design (San Diego, CA, USA) magnetic properties measurement system (MPMS) SQUID magnetometer. In the first experiment, 2.5 T SIRM was given in room temperature (300 K) and magnetization was measured continuously during zero-field (ZF) cycling from 300 to 10 K and back to 300 K in intervals of 5 K. In other experiments, SIRM was given at 10 K after the samples were cooled in ZF. Magnetization was monitored during ZF warming to 300 K in intervals of 5 K. In the third experiment, SIRM was given at 10 K after the samples had cooled in 2.5 T field. Magnetization was measured in intervals of 5 K while the samples were warmed back to 300 K in ZF.

Some samples were studied using Jeol JSM-5900LV (MA, USA) Scanning Electron Microscope (SEM) at the Geological Survey of Finland to further constrain the nature of the magnetic minerals. Four samples were studied by Digital Instruments (Santa Barbara, CA, USA) NANOSCOPE III Magnetic Force Microscope (MFM) in the IRM. The MFM uses a very fine magnetically coated tip mounted on a cantilever to measure magnetic force as it scans across the surface of a sample in room temperature and in field of 50 mT.

Table 1. Petrophysical properties of samples from the Vredefort and Johannesburg domes before and after lightning pulses.

Sample	Rock type	χ_O (10^{-6} SI)	NRM_O (mA m^{-1})	Q_O (−)	$SIRM_O$ (mA m^{-1})	REM_O (−)	I (kA)	χ_L (10^{-6} SI)	P_L	NRM_L (mA m^{-1})	Q_L (−)	$SIRM_L$ (mA m^{-1})	REM_L (−)
Vredefort dome													
LV4	Granite	5572	293	2.3	34 360	0.01	11.5	6981	1.05	13 563	86.8	28 790	0.47
LV42	Gneiss	3645	672	8.2	45 387	0.01	11.5	6826	1.17	9057	59.3	9280	0.98
LV47	Gneiss	6784	1093	7.2	49 847	0.02	11.5	7186	1.20	9825	61.1	14 480	0.68
Originally high Q value													
LV2	Granite–Gneiss	812	1412	78	1593	0.89							
LV17	Granite	2104	16 915	359	45 321	0.37							
Johannesburg dome													
HV50	Gneiss	286	69	10.8	246	0.28	17.9	428	1.03	498	51.9	693	0.72
HV51	Gneiss	373	64	7.7	818	0.08	17.8	532	1.05	293	24.6	602	0.49
HV53	Granodiorite	125	1	0.4	97	0.01	17.8	130	1.06	35	12.0	95	0.37
HV55	Granodiorite	148	69	20.8	282	0.24	16.3	91	1.05	113	55.7	158	0.72
HV57	Gneiss	201	69	15.3	320	0.22	16.7	180	1.09	100	24.8	116	0.86
HV58	Pegmatite	1496	17	0.5	471	0.04	17.8	7688	1.06	1470	8.5	3349	0.43
HV59	Migmatite	1088	266	10.9	6194	0.04	17.8	1737	1.33	3550	91.3	6153	0.58

Notes: Values are presented for same palaeomagnetic cylinder before and after lightning pulses. χ, magnetic susceptibility; P, degree of anisotropy: $P = K1/K3$, where $K1$, $K2$ and $K3$—mean AMS eigen vectors, which represent the maximum, intermediate and minimum susceptibility axis, respectively; NRM, natural remanent magnetization; Q Koenigsberger's ratio: $Q = \frac{J_R}{J_i} = \frac{\mu_0 \times NRM}{KH}$, where J_R —remanent magnetization, J_i—induced magnetization, μ_0—magnetic permeability ($4\pi 10^{-7}$ Tm^2 A^{-1}); H, magnetic field at the South Africa, used value 28 105 nT; REM = NRM/SIRM—ratio of natural remanent magnetization and saturation isothermal remanent magnetization, I, current during the high-voltage treatment (lightning simulations). O denotes original untreated samples. L denotes samples that were pulsed with current.

The resolution is high enough to allow imaging of the magnetization structure inside domain walls. For this, the samples were polished down to colloidal silica level and cut to fit the microscope (max. 1 × 1 cm). At first, the NRM of some grains in the samples were studied with MFM. After that 1 T SIRM was imparted and the same grains were restudied with MFM.

It is noteworthy that rocks are not homogenous material and they can be heterogeneous by centimetre scale. However, previous palaeomagnetic and rock magnetic measurements of different subsamples from one sample indicate that the magnetization within the samples studied here is similar being relatively low and homogeneous indicating homogenous magnetic mineralogy within the samples. When measuring magnetic properties (susceptibility versus temperature; high-temperature hysteresis; MPMS), we crushed rocks and were picking up the magnetic material to ensure the comprehensive representation of magnetic material.

3 RESULTS

3.1 Petrophysics and remanent magnetization

Palaeomagnetic and rock magnetic measurements of different subsamples from one sample indicate that the magnetization within the studied samples is similar indicating homogenous magnetic mineralogy within the samples. This is also confirmed by AMS study (Table 1). The degree of AMS (P = Kmax/Kmin) is low (<6 per cent) in majority of the samples (Hrouda 1982) that give the most important results for this study.

Values for petrophysical properties of the same cylinders before and after lightning pulses are listed in Table 1 and shown in Fig. 3. Lightning pulses enhanced Q values of all the studied samples from 0.4–20.8 to 8.5–91.3. Susceptibility values increased only slightly, but NRM values were one order of magnitude higher after lightning experiments. Sample HV58 was exception since also susceptibility increased fivefold and therefore the Q value did not increase so much.

Demagnetization of SIRM documents the nature of the magnetic phases in the rock and, hence, gives information about magnetic carriers, while the demagnetization of the NRM gives information about the nature and origin of magnetization (e.g. Cisowski & Fuller 1978). For example, we know that in magnetically fine-grained rocks a typical initial REM ratio (NRM/SIRM) for TRM acquired in geomagnetic field is of order 10^{-2} (Cisowski & Fuller 1978). REM ratios of 0.14–0.8, where NRM is harder than SIRM, have been reported for protolodestones (Wasilewski 1977, 1979; Wasilewski & Kletetschka 1999).

Intensity decay curves during AF demagnetization of NRM and SIRM before and after the lightning experiments for selected samples are shown in Fig. 4. These are shown also for two samples that have originally high Q values (LV17 and LV2) and have been hit by lightning strike at the field so NRM is produced by lightning strikes at the field and it is actually lightning-induced remanent magnetization (LIRM). Both NRM (being LIRM) and SIRM for granite sample LV17 were very stable against demagnetization. The Figs 4 and 5 also demonstrate that samples LV4 and HV58 with high REM values after lightning experiments were resistant against demagnetization being similar to behaviour of LV17. We also show examples of samples where pulse increased REM but that are less resistant to AF demagnetization (HV55 and HV57). In general, the SIRM was more resistant than NRM against AF demagnetization for most of the untreated samples whereas after lightning pulses, NRM (being

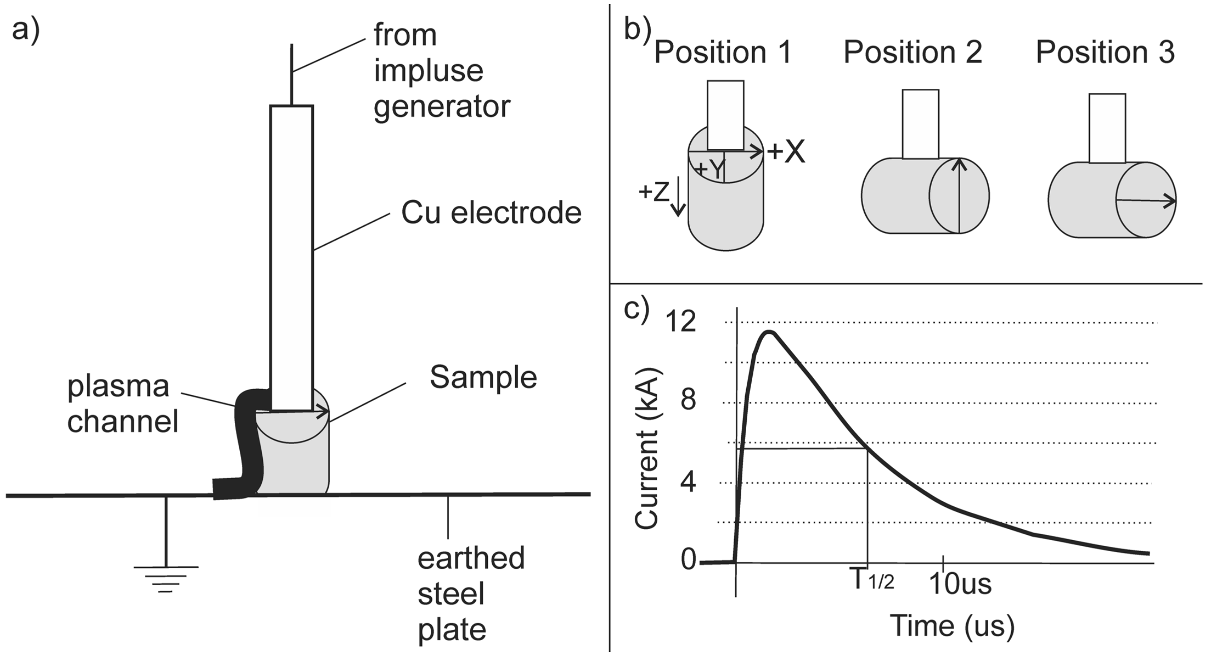

Figure 2. (a) Arrangements during the impulse current applications for the rock samples. (b) Orientation of the samples during the experiments. (c) Current during the experiments.

LIRM) was more resistant than SIRM or as resistant as SIRM for most of the samples (Table 1).

For all the samples, REM ratios increased due to the lightning pulses. REM values for the samples from the Vredefort increased to 0.47–0.98. The REM values of the untreated samples from Johannesburg fell in two groups (0.01–0.04 and 0.22–0.28); after lightning experiments the REM values increased to 0.37–0.58 and 0.72–0.86, respectively. For all the samples, the decay rate of REM ratio against demagnetizing field was more or less constant and the shape of the curve was similar for both the unpulsed and lightning pulsed samples.

3.2 Magnetic mineralogy—susceptibility versus temperature

Ferromagnetic minerals are most easily identified by their phase transitions (such as Curie points) and their Curie point temperature is easy to determine because of the large difference in moment between paramagnetic and ferromagnetic phases (e.g. Özdemir & Dunlop 2010). When pure, the minerals of interest in this study, magnetite and maghemite, have Curie temperatures of 580 and 645 °C, respectively (Özdemir & Banerjee 1984; Dunlop & Özdemir 1997). Due to variations of chemical composition (notably Ti-content), impurities and grain size, these temperatures vary. The formation of maghemite from magnetite can best be detected at LTs (Dunlop & Özdemir 1997). Observed Curie points and Verwey transition temperatures for our samples are listed in Table 2 and shown in Fig. 6. For example, Vredefort samples LV17 and LV2, which originally had high Q values, showed Hopkinson peaks at magnetite's Curie temperatures and higher intensity during the cooling than during the heating phase. Both samples showed a lower temperature (lower T) phase at *ca.* 150–380 °C during the heating, but not during the cooling. The low Verwey transition temperature (108 K) for sample LV17 indicates partially oxidized magnetite (Aragón *et al.* 1985; Özdemir & Dunlop 2010).

Lightning pulses had distinct effects to magnetic mineralogy of the samples from the Vredefort dome. Untreated reference samples (before lightning) from the Vredefort dome showed clear Hopkinson peaks and Curie points of 575–582 °C indicating presence of magnetite. After lightning pulses, Hopkinson peaks were slightly smeared out (sample LV4 does not exhibit it at all; Fig. 6f) and Curie points were increased to 583–590 °C, indicating maghemitization of magnetite (Özdemir & Dunlop 2010). After lightning pulses, the lower T phase was pronounced and this phase was not observed in the cooling curves, indicating that maghemite further transforms to haematite during the heating. Lightning pulses therefore seemed to produce maghemite in the magnetite containing samples. For samples from the Johannesburg dome, in some cases lightning pulses increased the temperature of the Curie point (e.g. HV52 and HV59) while in other cases Curie point was lowered (e.g. HV57). After lightning pulses, observed Hopkinson peaks (LV4, HV52, HV58 and HV59) diminished, which indicates that magnetite has altered to other minerals during lightning pulses and/or the grain size or the number of domain walls of minerals have been changed.

3.3 Magnetic mineralogy—remanent magnetization versus temperature

Heating to Curie points often alters the phases we are trying to identify. By studying the LT transitions of minerals, we can avoid the problems due to heating. Remanent magnetization of stoichiometric magnetite (Fe_3O_4) has two transitions below room temperature. The first one is the isotropic point ($T_i \approx 130$ K), where the first-order cubic magnetocrystalline anisotropy constant becomes zero. The second one is the Verwey transition (T_V) at *ca.* 120 K, in which the lattice structure changes from cubic to monoclinic (Özdemir & Dunlop 1999). Unlike magnetite pure maghemite (γ-Fe_2O_3) has no LT phase transition as seen in room temperature RT-SIRM cycling curve which is perfectly reversible on cooling and warming (Özdemir & Dunlop 2010). Recently, Özdemir & Dunlop (2010) determined tools for detecting partially oxidized magnetites. The first

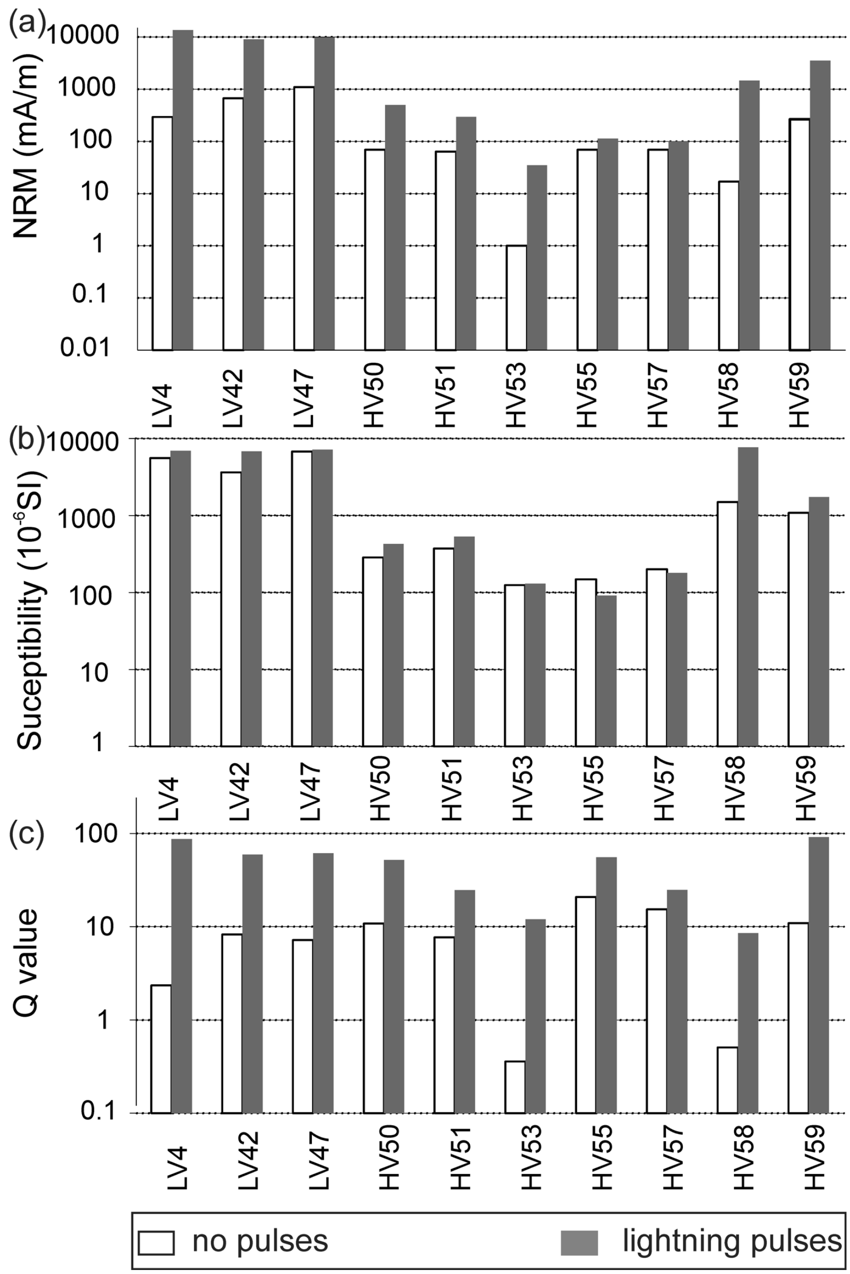

Figure 3. Petrophysical properties of samples from the Vredefort (LV) and Johannesburg (HV) domes before (white) and after lightning pulses (grey). Values are presented for same palaeomagnetic cylinder before and after lightning pulses. (a) Natural remanent magnetization values, (b) susceptibility values, (c) *Q* values (used field value 28 105 nT). Note the scale on *y*-axis is logarithmic. Samples are shown on *X*-axis.

hallmark of partial oxidation to maghemite is hump-shaped cooling and warming curves of RT-SIRMs while cycling through 300–10–300 K. The hump is due to a combination of the more or less linearly increasing moment of maghemite and the non-linearly decreasing moment of magnetite. This balance shifts depending on the degree of oxidation. The second hallmark is a shifted and broadened transition region of Verwey transition to lower temperatures. The third hallmark is that the oxidized minerals also recover more of the original RT-SIRM after cycling through 300–10–300 K than stoichiometric magnetite does. The fourth hallmark is a smeared-out Verwey transition and its shifting to lower temperatures when warming 10 K SIRM (2.5 T) after sample has been cooled to 10 K in ZF.

ZF warming curves of normalized LT SIRM (2.5 T in 10 K) for the unpulsed and lightning pulsed samples are shown in Fig. 7 and in Table 2. The $M_{\mathrm{SIRM}}/M_{\mathrm{SIRM(10)}}$ of the Vredefort sample LV2, which originally showed high *Q* values, decreased steadily from 50 to 300 K, and the Verwey transition was smeared out indicating the presence of oxidized magnetite. The lightning pulsed sample LV4 from the Vredefort showed two slightly broadened Verwey transitions and both Verwey transition temperatures were shifted to slightly higher temperatures compared to those of its unpulsed reference sample. The intensity of the shocked sample was 21 per cent lower than the intensity of the original sample. This indicates that lightning pulses have further oxidized magnetite in these samples.

Samples from the Johannesburg dome showed different behaviour during the LT SIRM experiments. Some samples (HV50, HV53, HV57 and HV58) showed clear differences between the untreated and lightning pulsed samples while the others (HV51, HV55

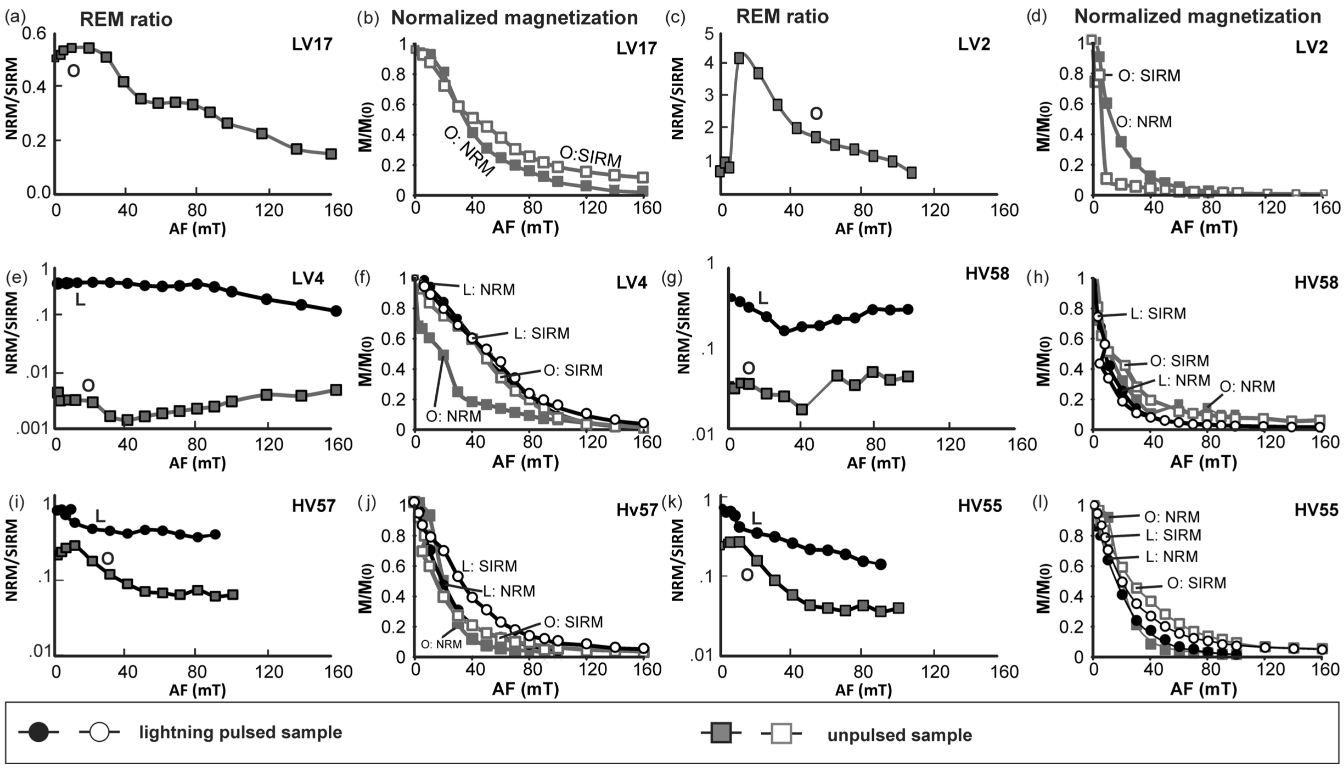

Figure 4. REM ratios (NRM/SIRM) as a function of alternating demagnetizing field and demagnetization curves for normalized O: NRM (natural remanent magnetization of a unpulsed reference sample), O: SIRM (saturation isothermal magnetization of a unpulsed reference sample), L: NRM (lightning-induced remanent magnetization of a pulsed sample) and L: SIRM (saturation isothermal magnetization on the sample that was hit pulsed by lightning strikes) of samples from Vredefort (LV) and Johannesburg (HV) dome. Black circles indicate samples treated with lightning pulses. Grey squares indicate original unpulsed samples. Closed (open) symbols indicate NRM (SIRM) in normalized diagrams. For samples LV17 and LV2, NRM is actually LIRM (lightning-induced remanent magnetization), since the samples were hit by lightning on the ground.

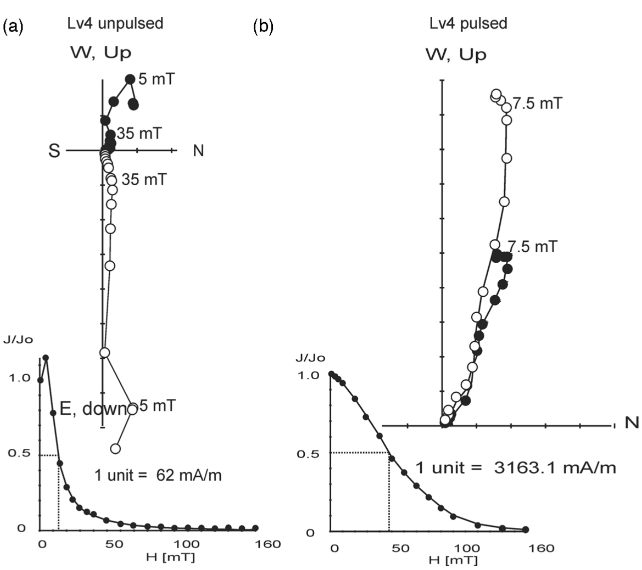

Figure 5. Orthogonal plot of AF demagnetization results and intensity decay curve for (a) unpulsed LV4 sample and (b) pulsed LV4 sample. Open and solid symbols are projections on vertical and horizontal planes, respectively.

and HV59) showed no differences. For example, the sample HV58 showed the most pronounced differences. Magnetization of the unpulsed reference sample decreased steadily from 20 to 95 K and then around T_V (107 K), 95 per cent of its magnetization was lost. After that, the curve was flat until 300 K. Its pulsed sister sample lost 35 per cent of its magnetization at 10–35 K and another 30 per cent at 35–120 K. At T_V, the intensity dropped more sharply, but the transition is smeared out compared to the original one. The pulsed samples from Johannesburg showed a sharper drop of intensity at 10–50 K than their unpulsed sister samples (Table 2). Özdemir & Dunlop (2010) have shown that this unblocking of SIRM during LTs between 10 and 50 K could imply *ca.* 10 nm grain sizes of oxidized magnetite, which can be associated with very fine scale cracking of the surface shell. In general, the pulsed samples showed slightly broadened and elevated T_Vs compared to the unpulsed reference samples (except for HV55, and HV57).

For sample LV2 with originally high Q values, the RT-SIRM cooling and warming curves were hump-shaped. There was neither a sign of the isotropic temperature T_i nor clear minimums in the curves, but there was a faint indicator of the Verwey transition in the warming curve at 50 K. Magnetization of the unpulsed reference sample LV4 showed a steady decrease during the cooling from 300 K, gradual at first and then more strong as T_V (102–106 K) was approached. In contrast, the pulsed sample LV4 showed hump-shaped cooling and heating curves, which reached a maximum at 200 K. Verwey transitions (96–107 K) were lower than those for the unpulsed LV4 sample, indicating maghemitization. The pulsed sample recovered more of the RT-SIRM (83 per cent) during the warming than its unpulsed sister sample (74 per cent). This is an additional proof for maghemitization since the internal stress due to lattice mismatch at the maghemite–magnetite interface plays a significant role in pinning the magnetite remanence and causing partial recovery in cycling through the Verwey transition. A fragmented maghemite shell would reduce the effective grain size and thus increase the magnetic memory (Özdemir & Dunlop 2010).

Table 2. Rock magnetic properties of lightning pulsed and unpulsed reference samples from Vredefort and Johannesburg domes, South Africa.

Sample	T_{v1} (K)	T_{v2} (K)	T_{c1} (°C)	T_{c2} (°C)	Hop, S	H/C	RT_{SIRM} cooling T_v (K)	RT_{SIRM} heating T_v (K)	Notes	FC T_v (K)	ZFC T_v (K)	M_{300}'	Notes
	Susceptibility versus T^a						Magnetization versus low T^b						
	VREDEFORT												
	NO LIGHTNING PULSES												
LV47 (R)	123			575	Hop, S	C							
LV4 (R)	128	109	160–390	582	Hop, S	C	102.0	105.8			101.9/123.6	0.74	
LV42 (R)							120.9	111.4			112.3/129.6	0.43	
HIGH Q IN SITU													
LV2	128		150–375	595	Hop, S	C	?	?	Hump, smeared		?	0.81	Smeared
LV17		108	145–385	565, 605	Hop	C							
	AFTER LIGHTNING PULSES												
LV47	123		250–415	585	Hop, S	C							
LV4	126	108	160–380	590	S	H	95.9	106.7	Hump	108.4/127.0	108.4/128.0	0.83	Hump
LV42	123		415	583	Hop	H	115.1	107.9		117.8	107.4	0.36	
	JOHANNESBURG												
	NO LIGHTNING PULSES												
HV50 (R)			250–390	561	S	C	95	95	Hump, smeared		99.1	0.66	
HV51 (R)							84	85	Hump, smeared	122.6	0.75		
HV53 (R)							94	94	Hump, smeared		127.4	0.64	
HV55 (R)			240–405	587		C	104	125			123.6	0.61	
HV57 (R)			280–420	580		C	125.8	120.0		106.5/123.1	106.6/121.2	0.39	
HV58 (R)	123	105	250–401	588	Hop	C	115.2	117.1			107.5	0.26	
				?									
HV59 (R)		116		580	Hop, S	C	110.5	112.5		112.3	112.3	0.43	
	LIGHTNING PULSES												
HV50				Smeared		C	99	99	Hump, smeared	Hump	123.5	0.66	Broadened fast:10–50K,
HV51							49	54	Hump, smeared	Hump	129.2	0.8	Fast:10–140K,
HV53							94	95	Hump, smeared		129.2	0.6	Fast:10–50K, hump
HV55			275–410			C	95	95			120.7	0.59	Fast:10–50K
HV57	121		346–440	570	Hop	C	111.5	113.5		112.6	112.6	0.35	Fast:10–50K
HV58				502, 584		C	104	105	Hump, smeared out		122.6	0.6	Broadened Verwey
HV59		114		588	Hop,S	C	105.9	116.9		118.2	118.2	0.41	

Notes: (R), Reference sample is a sister sample from the same core for the palaeomagnetic cylinder that was treated with lightning pulses. T_v, Verwey transition during the low-temperature treatment; T_c, Curie point during the high-temperature treatment; Hop, Hopkinson's peak observed; S, shoulder-type heating curve during high-temperature susceptibility measurement; H(C), intensity of heating (cooling) curve is higher; RT_{SIRM} – 2.5 T SIRM given in room's temperature (300 K): FC, field-cooling in 2.5 T field; ZFC, zero-field-cooling; M_{300}', memory of the magnetization given in 300 K and then cooled down to 10 K and heated back to 300 K.

[a]Masses of powdered samples for Curie point measurements were 0.5–0.8 g.

[b]Masses of powdered samples for MPMS were 0.3–0.45 g.

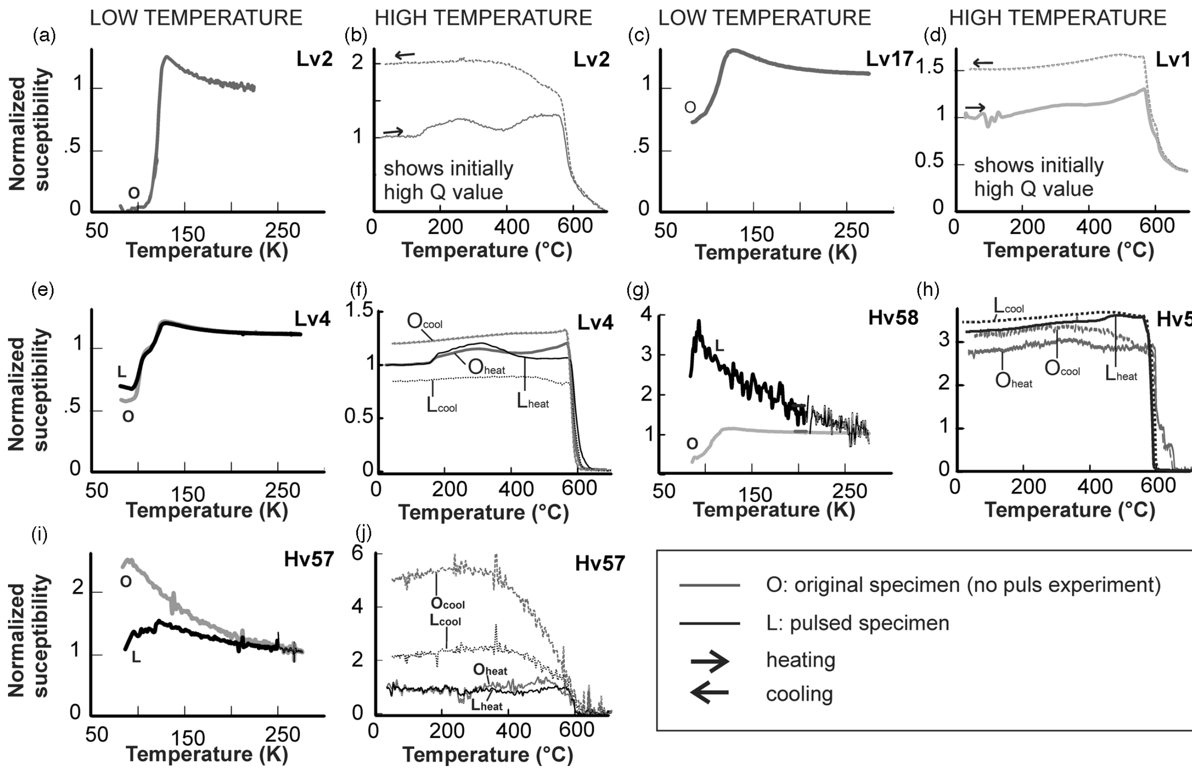

Figure 6. Normalized low and high-temperature thermomagnetic curves (susceptibility versus temperature) for samples from Vredefort (LV) and Johannesburg (HV) domes. L indicates sample treated with lightning pulses (black). O indicates original unpulsed samples (grey). Samples LV2 and LV17 have been hit by lightning strike on the field.

Samples from the Johannesburg dome showed different behaviour during the RT-SIRM experiments. Sample HV58 showed the most pronounced differences between the pulsed and unpulsed sister samples. The unpulsed sample showed typical curves for stoichiometric magnetite (Özdemir & Dunlop 2010) with an addition of reversed magnetization during the experiment at 104 K. The pulsed sister sample showed hump-shaped heating and slightly hump-shaped cooling curves indicating maghemitization. The pulsed sample recovered more (60 per cent) of the original remanence than the unpulsed sample (26 per cent). Samples HV57, HV53 and HV51 showed moderate changes during the RT-SIRM experiment due to the lightning. For example, T_V of sample HV57 shifted from 126 K for the untreated sample to 112 K for the pulsed sample. Samples HV59, HV55 and HV50 did not show any differences during the RT-SIRM experiment between lightning pulsed and unpulsed samples.

3.4 Hysteresis properties

Room temperature hysteresis properties of lightning treated and untreated samples were generally similar showing narrow hysteresis loops, which may be due to the fact that hysteresis properties were measured from the whole palaeomagnetic cylinders where the content of ferrimagnetic material is variable. Yet lightning pulsed sample shows threefold higher saturation remanent magnetization values. High-temperature hysteresis properties of the pulsed and unpulsed samples LV4 were measured in 25 °C intervals from room temperature to 600 °C. We detected the temperatures for changes from high-temperature susceptibility curves (Fig. 6) and show hysteresis loops for these temperatures. Increasing temperature reduced the coercivity and saturation magnetization (M_S) and narrowed the hysteresis loops of both samples (Fig. 8). The shape of the hysteresis loops of pulsed sample start to change at 500 °C while coercivity is still decreasing indicating the formation of new magnetic minerals, this is not obtained for unpulsed reference sample. Moreover, M_R of the pulsed sample increased after 275 °C, which could be indication of oxidized magnetites. Actually, similar shape to the curve of pulsed samples has been earlier observed for oxidized magnetites (e.g. Wasilewski 1977).

3.5 Microscope studies

SEM analyses of magnetic grains (>µm) of the sample LV4 (pulsed and unpulsed reference sample) show two types of magnetite grains. Some of them had typical magnetite shape (Figs 8b and e) and the others had irregular atypical shape for magnetite (Figs 8c and f). We show two examples of magnetic grains of unpulsed sample LV4. Fig. 8(b) shows an example of *ca.* 25 µm magnetite with typical shape that has few cracks and Fig. 8(c) shows larger (>100 µm) magnetite with several microfractures. Two examples are also shown for pulsed sample LV4. Fig. 8(e) shows *ca.* 40 µm magnetite with typical shape that has several microfractures and Fig. 8(f) shows smaller atypical shaped grain with several microfractures. Majority of the grains were fractured in both pulsed and unpulsed sample. Magnetite shaped samples in unpulsed sample seemed to have less microfractures than in pulsed sample. Due to magnification limitations of the SEM, we were not able to study smaller than µm sized grains.

MFM studies of Vredefort sample LV4 showed that the few observable magnetic grains in both the pulsed and unpulsed samples did not have any lamellae structure, but the structure was fragmented. Moreover, the lightning pulsed sample showed reduced

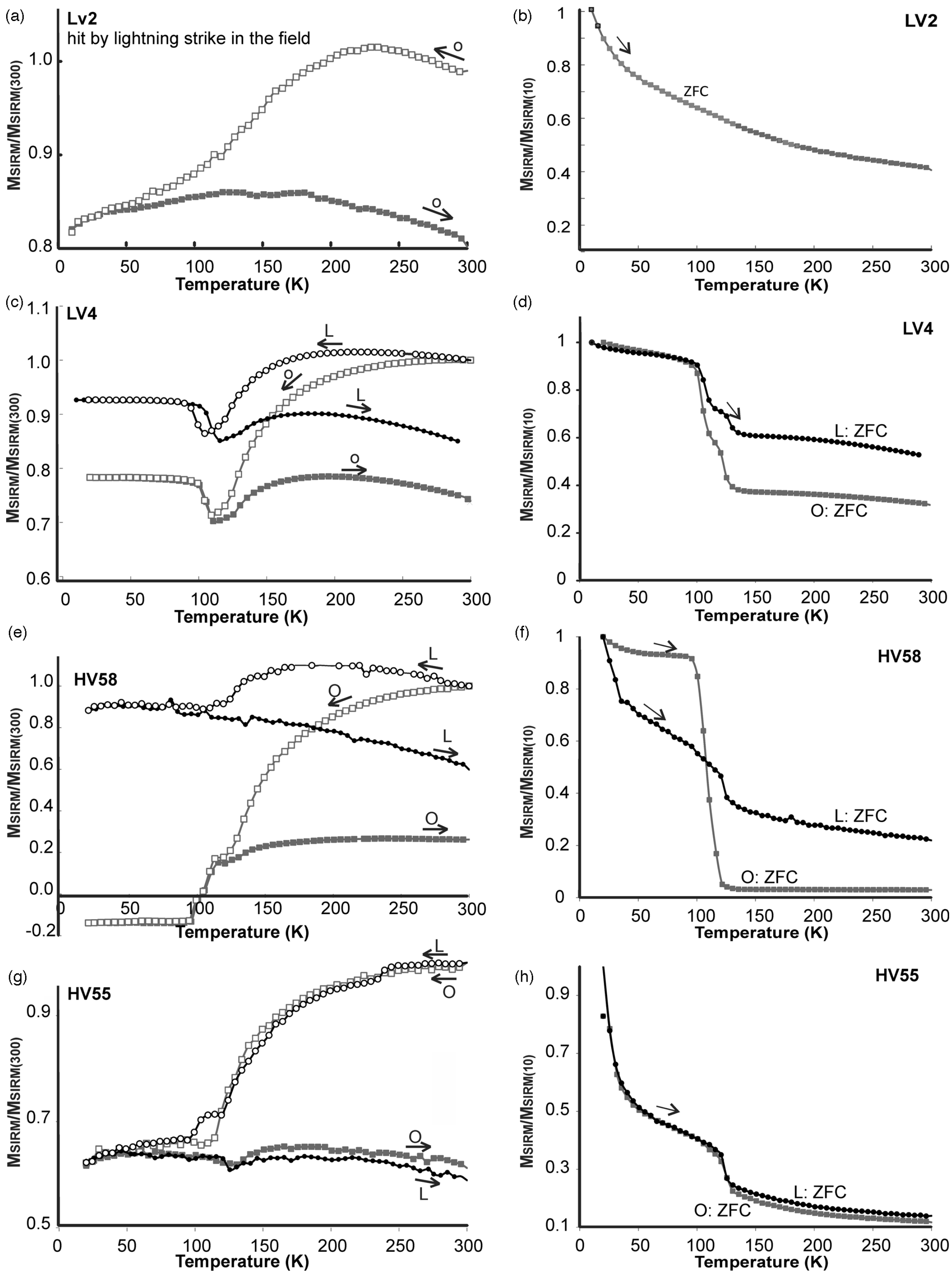

Figure 7. Diagrams on a left side show zero-field cooling and rewarming curves of SIRM (saturation isothermal remanence) produced at 300 K. Diagrams on a right side show zero-field warming curves of SIRM produced at 10 K after zero-field cooling from 300 K (ZFC). Black indicates sample treated with lightning strike pulses (L). Grey indicates original unpulsed samples (O). Sample LV2 has been hit by lightning strike on the field.

effective grain size. This was noted when imaging the samples perpendicular to scanning surface after giving to them 1 T IRM. It is evident that these samples that had fragmented magnetic grain structure were capable of being strongly magnetized by lightning and lightning reduced the effective grain size.

4 DISCUSSION

Large lightning field produced high NRM values in all studied samples and slightly enhanced susceptibility (Fig. 3). The lightning treated samples revealed high Q values. Also, their REM

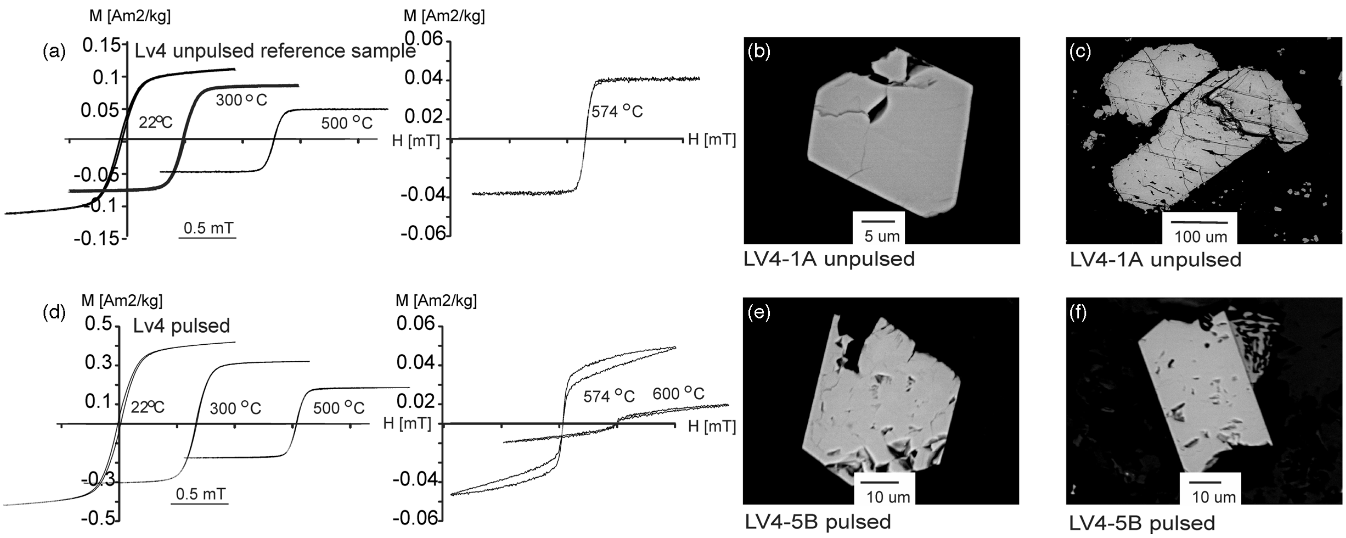

Figure 8. Hysteresis curves at different temperatures (a, d) and scanning electron microscope (SEM) images (b, c, e, f) for unpulsed and lightning pulsed sister specimens from the same sample.

(NRM/SIRM) ratios increased due to lightning pulses, reaching values observed for lodestones and for protolodestones (Wasilewski 1977, 1979). However, it is puzzling that in most samples IRM values seem to decrease after lightning pulses, which is contradictory to generation of lodestones.

However, we observed several hallmarks of maghemitization (Özdemir & Dunlop 2010) for some of the lightning pulsed samples during the LT variation of the IRM whereas some samples did not show changes. For example, the pulsed samples showed hump-shaped cooling and heating curves of RT-SIRM, and slightly broadened and smeared out Verwey transitions, and it's shifting to lower Verwey temperatures (Fig. 7). The pulsed samples lost magnetization more rapidly at 20–50 K than the unpulsed samples did. Özdemir & Dunlop (2010) have shown that this unblocking of SIRM during LTs between 10 and 50 K imply *ca.* 10 nm sizes, which can be associated with very fine scale cracking of the maghemite surface shell. The pulsed samples recovered more of the original RT-SIRM than the unpulsed samples, which is an additional proof for maghemitization since the internal stress due to lattice mismatch at the maghemite–magnetite interface plays a significant role in pinning the magnetite remanence and causing partial recovery in cycling through the Verwey transition. This is an additional evidence for a fragmented magnetite shell that would reduce the effective grain size and so increase the magnetic memory (Özdemir & Dunlop 2010). Further indication of changes in magnetic mineralogy due to lightning pulses came from thermomagnetic curves. In case of samples LV2 and LV17 that had been hit by lightning strike at the field, high-temperature measurements indicate presence of maghemite (Fig. 6*)*. In case of some pulsed subsamples, Curie points increased (to 583–605 °C) slightly above the Curie point of magnetite (580 °C) and Hopkinson peaks in susceptibility (*T*) curves were slightly smeared off (Fig. 6f) indicating partially oxidized magnetite (Özdemir 1990). Moreover, the lower T (200–400 °C) phase in the susceptibility versus temperature measurement became pronounced after the lightning. These changes are interpreted to indicate further oxidation of magnetite (maghemitization). The change in magnetic mineralogy in case of some samples is also shown by high-temperature hysteresis properties (Fig. 8).

However, we note here that changes in magnetic mineralogy were not obtained for all of the studied samples and these experiments show that lightning phenomenon is complicated. Based on SEM analyses, we suggest that lightning pulses partially further oxidized magnetite to maghemite in the samples where magnetite grains contained microfractures before the tests. We propose that due to very high temperatures and energy released during the lightning pulse this fracturing was enhanced. Results from magnetic microscope studies are not conclusive, but they support the fact that the intense NRM values are associated with the highly irregular microstructure within the magnetic grains. Already in 1953, Graham suggested that high stability of remanence could be a subdivision of mineral grains into magnetite, maghemite and non-magnetic ilmenite (e.g. Tucker & O'Reilly 1980). Moreover, previous studies have shown that magnetic susceptibility and NRM can be enhanced several times because of the formation of small (nanocrystalline) magnetite and/or maghemite (e.g. Harrison *et al.* 2002; McEnroe *et al.* 2002). For example, Banfield *et al.* (1994) proposed a connection between intergrown structure of massive magnetite–maghemite at the nanometer scale and its strong magnetic property and later McEnroe *et al.* (2002) pointed out that the mechanism explaining the magnetic anomaly in massive ilmenite rock was the formation of nanometer-scale lamella of haematite and ilmenite during the exsolution of haematite–ilmenite solid solution.

The aim of these experiments was to find out the reason for the observed intense NRM in the Vredefort rocks. For a long time, it has been suggested that the source for elevated NRM values is related to an impact event, in which an ultra-small SD magnetite forms in a high-pressure/temperature environment and crystallizes along planar deformation features (Hart *et al.* 1995, 2000; Cloete *et al.* 1999). Carporzen *et al.* (2005) further proposed that a plasma field randomized the directions of remanent magnetization (Carporzen *et al.* 2005). Salminen *et al.* (2009) showed that there is no direct impact link to explain the high NRM values. Since the Johannesburg dome samples, being far away from Vredefort, also reveal high *Q* values. Furthermore, by drilling two 10 m holes in Vredefort rocks, Carporzen *et al.* (2012) found that abnormal magnetization is only a surface (upper 0.5 m) feature, which does not support an impact origin for high *Q*. Since lightning strikes are known to produce intense NRM values, they were a more likely explanation for high NRM values and often their random orientations in the Vredefort when also taking in to account that the lightning strike activity in South Africa is known to be high. Lightning strikes are thought to produce intense magnetization (e.g. Cox 1961; Dunlop *et al.* 1984; Verrier & Rochette 2002) and in the case of lodestones to produce intense and hard remanent magnetization (Wasilewski 1977, 1979; Banfield *et al.* 1994; Wasilewski & Kletetschka 1999). We have shown by studying several rock magnetic properties of samples from Vredefort and Johannesburg that were artificially hit by lightning pulses (11.5–18 kA) that lightning strikes can indeed enhance magnetic properties of the samples. We propose that is at least partly due to oxidized magnetites that contain microstructures.

5 CONCLUSIONS

Laboratory made lightning strikes can produce intense magnetizations and can therefore be the cause for the observed high Q values in rocks from Vredefort as well as from Johannesburg domes. Results from this study show that lightning phenomenon is complicated. However, petrophysical properties, LT magnetization measurements and the temperature variation of susceptibility showed that lightning pulses changed the magnetic mineralogy of some of the studied samples. These lightning induced changes include enhanced NRM and susceptibility values, increased Curie points, more pronounced low T phases appearing in susceptibility versus temperature curve, and changes in hysteresis properties during high-temperature measurements. The main finding from this study comes from LT versus magnetization (MPMS) measurements, which support that lightning strikes partially oxidize magnetite in some of the samples as seen in as broadened and smeared out Verwey transitions, shifting of Verwey temperatures to lower, and hump-shaped cooling and heating curves of 300 K SIRM. SEM study shows that these changes are observed in the samples that contained microfractures already before experiments.

ACKNOWLEDGEMENTS

We thank two anonymous reviewers for their constructive comments which improved this paper. JS appreciates the help and discussions with the whole stuff in IRM during and special thanks to Mike Jackson who guided her through two visits in IRM. Finnish Cultural Foundation, Emil Aaltonen Foundation and Academy of Finland are thanked for financial support for JS. Dr Marja Lehtonen (geological Survey of Finland) is thanked for her help with SEM. Miss Florence Loi's help with language is appreciated.

REFERENCES

Aragón, R., Buttrey, D.J., Shepherd, J.P. & Honig, J.M., 1985. Influence of nonstoichiometry on the Verwey transition, *Phys. Rev. B.,* **31,** 430–436.

Banfield, J.F., Wasilewski, P.J. & Veblen, D.R., 1994. TEM study of realtionships between the microstructures and magentic properties of strongly magnetized magnetite and maghemite, *Am. Mineral.,* **79,** 654–667.

Carporzen, L., Gilder, S.A & Hart, R.J., 2005. Palaeomagnetism of the Vredefort meteorite crater and implications for craters on Mars, *Nature,* **435,** 198–201.

Carporzen, L., Gilder, S.A. & Hart, R.J., 2006. Origin and implications of Verwey transitions in the basement rocks of the Vredefort meteorite crater, South Africa, *Earth planet. Sci. Lett.,* **251,** 305–317.

Carporzen, L., Weiss, B.P., Gilder, S.A., Pommiear, A. & Hart, R.J., 2012. Lightning remagnetization of the Vredefort impact crater: no evidence for impact generated magnetic fields, *J. geophys. Res.,* **117,** E01007, doi:10.1029/2011JE002919.

Cawthorn, R.G., Eales, H.V., Walraven, F., Uken, R. & Watkeys, M.K., 2006. The Bushveld complex, in *The Geology of South Africa,* Chapter 11, pp. 261–281, eds Johnson, M.R., Annhaeusser, C.R. & Thomas, R.J., Geological Society of South Africa.

Christian, H.J. *et al.*, 2003. Global frequency and distribution of lightning as observed from space by the Optical Transient Detector, *J. geophys. Res.,* **108**(D1), 4005, doi:10.1029/2002JD002347.

Cisowski, S.M. & Fuller, M., 1978. The effect of shock on the magnetism of terrestrial rocks, *J. geophys. Res.,* **83,** 3441–3458.

Cloete, M., Hart, R.J., Schmid, H.K., Drury, M., Demanet, C.M. & Sankar, K.V., 1999. Characterization of magnetite particles in shocked quartz by means of electron- and magnetic force microscopy: Vredefort, South Africa, *Contrib. Mineral. Petrol.,* **137,** 232–245.

Cox, A., 1961. *Anomalous Remanent Magnetization of Basalt,* 38pp., U.S. Geological Survey Bulletin, 1083-E., U.S. Geological Survey, Washington, DC.

Crawford, D.A. & Schultz, P.H., 1999. Electromagnetic properties of impact-generated plasma, vapor and debris, *Int. J. Impact Eng.,* **23,** 169–180.

Dunlop, D.J. & Özdemir, Ö., 1997. *Rock Magnetism, Fundamentals and Frontiers,* Cambridge University Press, Cambridge, England, 573pp.

Dunlop, D.J., Schutt, L.D. & Hale, C.J., 1984. Paleomagnetism of Archean rocks from northwestern Ontario: III. Rock magnetism of the Shelley Lake granite, Quetico Subprovince, *Can. J. Earth Sci.,* **21,** 879–886.

Eriksson, P.G., Altermann, W. & Hartzer, F.J., 2006. The Traansvaal Supergroup and its precursors, in *The Geology of South Africa,* pp. 237–260, eds Johnson, M.R., Annhaeusser, C.R. & Thomas, R.J., Geological Society of South Africa.

Flowers, J.W., 1943. The channel of the spark discharge, *Phys. Rev.,* **64,** 225–235.

Gibson, R.L. & Reimold, W.U., 2001. *The Vredefort Impact Structure: South Africa (The Scientific Evidence and a Two-Day Excursion Guide)*. Memoir 92 Council for Geoscience Pretoria, 110pp.

Gibson, R.L. & Reimold, W.U., 2008. *Geology of the Vredefort Impact Structure: A Guide to Sites of Interest*. Council for Geoscience, Pretoria, Memoir XX Council for Geoscience Pretoria, 97, 181p.

Graham, K.W.T., 1961. The remagnetization of a surface outcrop by lightning currents, *Geophys. J. Int.,* **6,** 85–102.

Hargraves, R.B., 1961. Shatter cones in the rocks of the Vredefort ring, *Trans. geol. Soc. South Afr.,* **64,** 147–161.

Hargraves, R.B., 1970. Paleomagnetic evidence relevant to the origin of the Vredefort ring, *J. Geol.,* **78,** 253–263.

Harrison, R.J., Dunin-Borkowski, R.E. & Putnis, A., 2002. Direct imaging of nanoscale magnetic interactions in minerals, *Proc. Natl. Acad. Sci. U.S.A.,* **99,** 16 556–16 561.

Hart, R.J., Hargraves, R.B., Andreoli, M.A.G., Tredoux, M. & Doucouré, C.M., 1995. Magnetic anomaly near the center of the Vredefort structure: Implications for impact-related magnetic signatures, *Geology,* **23,** 277–280.

Hart, R.J., Connell, S.H., Cloete, M. & Mare, L., 2000. 'Super magnetic' rocks generated by shock metamorphism from the centre of the Vredefort impact structure, South Africa, *South Afr. J. Geol.,* **103,** 151–155.

Hattingh, P.J., 1989. The paleomagnetism of the upper zone of Bushveld Complex, *Tectonophysics,* **165,** 131– 142.

Hattingh, P.J., 1999. Palaeomagnetism and the Bushveld Complex in Southern Africa: some enigmas, in *The Indian Subcontinent and Gondwana: A Palaeomagnetic and Rock Magnetic Perspective,* pp. 1–7, eds Radhakrishna, T. & Piper, J.D.A., No. 44, Memoir-Geol. Soc. India.

Henkel, H. & Reimold, W.U., 1998. Integrated geophysical modelling of a giant, complex impact structure: anatomy of the Vredefort structure, South Africa, *Tectonophysics,* **287,** 1–20.

Hrouda, F., 1982. Magnetic anisotropy of rocks and its application in geology and geophysics, *Geophys. Surv.,* **5,** 37–82.

Ivanov, B.A., 2005. Numerical modeling of the largest terrestrial meteorite craters, *Solar Syst. Res.,* **39,** 381–409.

Jackson, G.M., 1982. Paleomagnetic study and magnetic modelling of the Vredefort dome, Project for Honours requirement, University of Witwatersrand, Johannesburg, RSA, 40pp.

Kamo, S.L., Reimold, W., Krogh, T.E. & Colliston, W., 1996. A 2.023 Ga age for the Vredefort impact event and a first report of shock metamorphosed zircons in pseudotachylitic breccias and granophyre, *Earth planet. Sci. Lett.,* **144,** 369–387.

Krider, E. & Roble, R.E., 1986. *The Earth's Electrical Environment,* National Academy Press, Washington DC, 263pp.

Layer, P.W., Kröner, A., McWilliams, M. & Clauer, N., 1988. Regional magnetic overprinting of Witwatersrand Supergroup sediments, South Africa, *J. geophys. Res.,* **93,** 2191–2200.

Layer, P.W., Kröner, A., McWilliams, M. & York, D., 1989a. Elements of the Archaen thermal history and apparent polar wander of the eastern Kaapvaal Craton, Swaziland, from single grain dating and paleomagnetism, *Earth planet. Sci. Lett.,* **93,** 23–34.

Layer, P.W., Kröner, A., McWilliams, M. & Burghele, A., 1989b. Paleomagentism and age of the Archean Usushwana complex, southern Africa, *J. geophys. Res.,* **93,** 449–458.

McEnroe, S.A., Harrison, R.J., Robinson, P. & Langenhorst, F., 2002. Nanoscale haematite–ilmenite lamellae in massive ilmenite rock: an example of 'lamellar magnetism' with implications for planetary magnetic anomalies, *Geophys. J. Int.,* **151,** 890–912.

Muundjua, M., Hart, R.J., Gilder, S.A., Carporzen, L. & Galdeano, A., 2007. Magnetic imaging of the Vredefort impact crater, South Africa, *Earth planet. Sci. Lett.,* **261,** 456–468.

Özdemir, Ö., 1990. High-temperature hysteresis and thermoremanence of single-domain maghemite, *Phys. Earth Planet. Int.,* **65,** 125–136.

Özdemir, Ö. & Banerjee, S.K., 1984. High temperature stability of maghemite (γ Fe_2O_3), *Geophys. Res. Lett.,* **11,** 161–164.

Özdemir, Ö. & Dunlop, D.J., 1999. Low-temperature properties of a single crystal of magnetite oriented along principal magnetic axis, *Earth planet. Sci. Lett.,* **165,** 229–239.

Özdemir, Ö. & Dunlop, D.J., 2010. Hallmarks of maghemitization in low-temperature remanence cycling of partially oxidized magnetite nanoparticles, *J. geophys. Res.,* **115,** B02101, doi:10.1029/2009JB006756.

Reimold, W.U. & Gibson, R.L., 1996. Geology and evolution of the Vredefort impact structure, South Africa, *J. Afr. Earth Sci.,* **23,** 125–162.

Salminen, J., Pesonen, L.J., Donadini, F., Reimold, W.U. & Gibson, R.L., 2009. Paleomagnetic and rock magnetic study of the Vredefort impact structure and the Johannesburg Dome, Kaapvaal Craton, South Africa: implications for the apparent polar wander path of the Kaapvaal craton during the Mesoproterozoic, *Precambrian Res.,* **168,** 167–184.

Tucker, P. & O'Reilly, W., 1980. The laboratory simulation of deuteric oxidation of titanomagnetites: effect on magnetic properties and stability of thermoremanence, *Phys. Earth planet. Inter.,* **23,** 112–133.

Turtle, E.P. & Pierazzo, E., 1998. Constraints on the size of the Vredefort impact crater from numerical modeling, *Meteorit. planet. Sci.,* **33,** 483–490.

Wasilewski, P.J., 1977. Magnetic and microstructural properties of some lodestones, *Phys. Earth planet. Inter.,* **15,** 349–362.

Wasilewski, P.J., 1979. Lodestone-explanation for magnetic properties characterization of the source of magnetic hardening, *J. appl. Phys.,* **50,** 2428–2430.

Wasilewski, P.J. & Kletetschka, G., 1999. Lodestone: natures only permanent magnet—what it is and how it gets charged, *Geophys. Res. Lett.,* **26,** 2275–2278.

Verrier, V. & Rochette, P., 2002. Estimating peak currents at ground lightning impacts using remanent magnetization, *Geophys. Res. Lett.,* **20**(18), 1867, doi:10.1029/2002GL015207.